J Fluoresc (2014) 24:917–924
DOI 10.1007/s10895-014-1372-5

ORIGINAL PAPER

Targeted Singlet Oxygen Generation Using Different DNA-Interacting Perylene Diimide Type Photosensitizers

Haluk Dinçalp · Şevki Kızılok · Sıddık İçli

Received: 4 December 2013 / Accepted: 24 February 2014 / Published online: 5 March 2014

Abstract Singlet oxygen quantum yields (Φ_Δ) of different perylene diimides (PDIs) containing phenyl (**PDI-Ph**), pyrene (**PDI-Pyr**), and indole (**PDI-In**) units in bay positions of the ring were determined using 1,3-diphenylisobenzofuran (DPBF) method in toluene/methanol (99:1) system. Pyrene-substituted PDI were the most efficient singlet oxygen generator among the investigated photosensitizers with a quantum yield of Φ_Δ=0.93 in toluene/methanol. Additionally, their binding affinities to G-quadruplex DNA structure were investigated by steady-state measurements. There were marked red shifts of absorbance bands for **PDI-Pyr**/DNA strand complexes with respect to the absorption maxima of DNA-free solution of **PDI-Pyr** in phosphate buffer at pH 6.

Keywords Perylene diimide · Pyrene · Charge transfer · G-quadruplex DNA · Singlet oxygen · DPBF method

Introduction

One of the more novel and beneficial application of singlet oxygen in medicine is the cure of tumors. Today, photodynamic therapy (PDT) has become a potential candidate for the major utilization in the modern operation of cancer [1–4]. Singlet oxygen and other reactive oxygen species generated during the PDT processes can potently damage to tumor cells. These species are formed by the excitation of the special photosensitizers under visible light irradiation within tumor tissues in the presence of molecular oxygen [5].

Hematoporphyrin derivatives, a mixed composition of different porphyrins, are widely used photosensitizers in PDT. Porphyrins have gained some special properties such as high singlet oxygen production capacities, good solubilities in water, long wavelength absorptions and high extinction coefficients in visible region for PDT applications [5–8]. Another novel potential candidate for PDT applications is PDI derivatives [9], chemically more suitable photosensitizers with respect to porphyrins. PDIs are reviewed in versatile dyes and pigments class because of their excellent photochemical properties. PDIs are used mainly in high technological applications such as solar cells [10, 11], organic light-emitting diodes [12], organic field-effect transistors [13] and molecular switches [14]. Because of their long wavelength absorptions [15], high extinction coefficients in visible region [16], good singlet oxygen formation efficiencies [17, 18], and good photo [19] and chemical stabilities [20], they are currently used in both G-quadruplex stabilization [21, 22] and telomerase inhibition in cancer cells [23]. Their absorption spectra cover the 400–450 nm and 500–700 nm regions which are more crucial ranges for absorption of the solar photons which then initiates the singlet oxygen production by energy or electron transfer processes. An effective light absorption of the photosensitizer in tissues is a serious problem to overcome sufficient excitation. PDIs with high molar extinction coefficients and near-infrared absorbing properties are also good candidates for this purpose in PDT applications.

Activity of human telomerase, which is responsible for growth of cancer cells, is high level in most tumor tissues [24]. Telomerase accelerates the uncontrolled growth of tumor cells by adding DNA back to the telomeres [25]. Guanosines at the end of the telomeres are critical structures for maintaining the telomeres [26]. When the box-like structure of guanosines decomposes, the chromosomes start to unravel. G-

H. Dinçalp (✉) · Ş. Kızılok
Department of Chemistry, Faculty of Arts and Science, Celal Bayar University, Muradiye 45030, Manisa, Turkey
e-mail: haluk.dincalp@cbu.edu.tr

S. İçli
Solar Energy Institute, Ege University, Bornova 35100, Izmir, Turkey

quadruplex formation directly inhibits telomerase elongation in vitro [27].

Targeted photodynamic therapy is a new strategy that aims to direct the photosensitizers specifically towards the tumor tissues to enhance the efficiency and specificity of PDT. Tumor selectivity of the photosensitizer in tissues is essential point to get good results for PDT applications, otherwise undesirable location of the drug in healthy tissues causes some photoallergic or phototoxic reactions. There are different strategies to overcome the specific accumulation of the drugs at desirable location of the tumor tissues. In these techniques, the drugs can be conveyed to the target cells when they combine with specific ligands [28]. One of the pathways is the use of G-quadruplex as a drug carrier to target cancer cells for PDT. Shieh et al. have reported the binding affinity of porphyrin to the G-quadruplex aptamer conjugates and investigated the delivery of porphyrin sensitizer into cancer cells. The results have showed that the G-quadruplex-porphyrin complex exhibits a higher porphyrin accumulation in breast cancer cells than in normal epithelium cells. After treated with light for 180 s, the photodamage in cancer cells has been larger than in normal cells [29]. This is a good tactic for targeted photodynamic therapy. Also, the oxygen concentration in tumor tissue is a critical point for obtaining the desired photosensitization. Singlet oxygen and other reactive oxygen species could more potently kill diseased cells.

Taking into account the requirements for an effective PDT agent, we plan to synthesize new G-quadruplex stabilizers, mainly composed of unsymmetrical PDIs with phenyl, pyrene or indole units as shown in Fig. 1. Defect structure of chromosomes is a target area for PDI structure. We expect that singlet oxygen quantum yields of these combined agents will increase because pyrene [30] and indole [31] units can improve the singlet oxygen generation efficiency. Substitution at the bay positions of the ring improves the solubility of the agent. By using these unsymmetrical PDIs, preferred localization in the defect structure of tissues is expected. We have studied herein the singlet oxygen generation capacities of the agents and investigated the binding affinities of dyes to G-quadruplexes in phosphate buffer solution at pH 6.

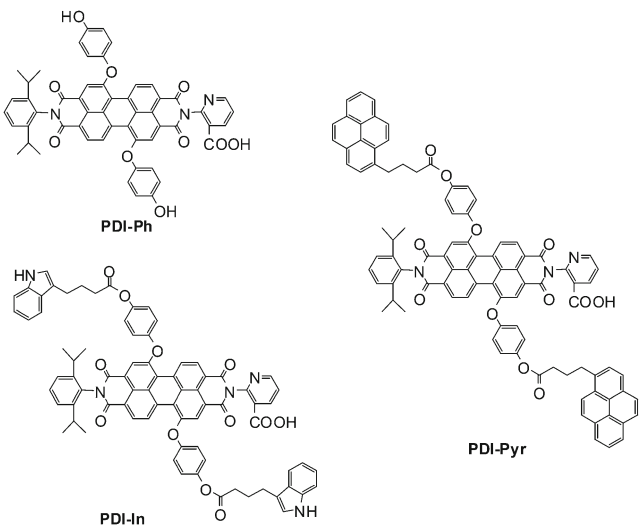

Fig. 1 Structural formulas of the studied dyes

Experimental Section

General Procedures

N-(2,6-diisopropylphenyl)-N′-(3-carboxy-2-pyridyl)-1,7-bis (4-hydroxyphenoxy)perylene-3,4,9,10-tetracarboxylic diimide (**PDI-Ph**), N-(2,6-diisopropylphenyl)-N′-(3-carboxy-2-pyridyl)-1,7-bis{4-[(4-pyrene-1-ylbutanoyl)oxy]phenoxy}perylene-3,4,9,10-tetracarboxylic diimide (**PDI-Pyr**), and N-(2,6-diisopropylphenyl)-N′-(3-carboxy-2-pyridyl)-1,7-bis{4-[(4-indole-3-ylbutanoyl)oxy]phenoxy}perylene-3,4,9,10-tetracarboxylic diimide (**PDI-In**) dyes were synthesized as described previously [32] and used as PDT agents in experiments. Solvents used in the spectroscopic studies were of spectrophotometric grade.

The five oligonucleotides were used to define the G-quadruplex DNA binding selectivity of the ligands. These oligonucleotides were single-stranded DNA (ss-DNA) [d(TTT TTT)], double-stranded DNA (ds-DNA) [d(CGC GCG ATA TCG CGC G)]$_2$, intermolecular G-quadruplex DNA (G4-DNA) [d(TAG GGT TA)]$_4$, intramolecular G-quadruplex DNA (G4′-DNA) [d(TTA GGG)$_4$] and dimeric hairpin quadruplex DNA (hp-DNA) [d(GGG GTT TTG GGG)]$_2$. The oligonucleotides were synthesized on a Thermo Electron DNA synthesizer and purified by reversed phase HPLC.

Determination of Singlet Oxygen Quantum Yields (Φ_Δ)

Singlet oxygen quantum yields were obtained by the measurement of DPBF degradation in the presence of the dyes under photolysis with reference to that of the same conditions of Methylene Blue photosensitizer (Φ_Δ=0.51) [33] in toluene/methanol (V/V = 99:1) solvent system. Irradiation was done in a PTI QM1 fluorescence spectrophotometer equipped with a Xe lamp at the excitation wavelength of 510 nm for 50 min. UV–visible measurements were performed with a JASCO V-530 UV–vis spectrophotometer. All the experiments were carried out at 25 °C.

DNA Preparation

DNA solution was prepared in below manner given in the literature [34]. Phosphate buffer solution was prepared in a H_2O/acetone (V/V = 95:5) solution. Oligonucleotides were dissolved in a 70 mM potassium phosphate/100 mM

potassium chloride/1 mM EDTA buffer at pH 6 (170 mM phosphate buffer), and then heated to 95 °C in a water bath for 3 min. Then, the solution was cooled to room temperature.

Two micromolar of each of the G-quadruplex structures was added to the solution of about 2 μM of the ligand. The total volume was equal to 3 mL. Then, the reaction vessels were transferred into an incubator where they remained for 2 h at 37.2 °C. After the incubation, UV–vis absorption spectra of the G-quadruplex-ligand complexes were compared to the nucleotide free solution of every ligand in phosphate buffer solution at pH 6.

Calculation of Binding Constants

Values of binding constants (K) of the ligands to the appropriate sites of the **PDI-Pyr** dye were calculated based on light absorption of the ligands at wavelength of 351 nm (Soret maximum) from the Eq. 1 given below [35]:

$$\frac{r}{C_f} = nK - Kr \quad (1)$$

where r is the number of moles of **PDI-Pyr** dye bound to one mol of G-quadruplex DNA structure, C_f is the concentration of free dye and n is the number of equivalent binding sites. r is calculated from the Eq. 2 [35, 36],

$$r = \frac{C_b}{C_{DNA}} \quad (2)$$

where C_b is the concentration of bound perylene dye and C_{DNA} is the nucleotide concentration. Also, concentration of free perylene dye (C_f) was calculated from the Eqs. 3 and 4 given below [36]:

$$C_f = C \times (1-\alpha) \quad (3)$$

$$C_b = C - C_f \quad (4)$$

where C is the total perylene dye concentration (2 μM). α, the fraction of bound perylene dye, was calculated using the Eq. 5 [36],

$$\alpha = \frac{A_f - A}{A_f - A_b} \quad (5)$$

where A_f and A_b are the absorbance of the free and fully bound perylene dye at 351 nm, respectively and A is the absorbance at 351 nm at any given point during the titration.

Results and Discussion

Vis Absorption and Fluorescence Emission Properties

Normalized steady-state absorption and fluorescence emission spectra of **PDI-Pyr** dye in 170 mM phosphate buffer solution at pH 6 (70 mM potassium phosphate/100 mM potassium chloride/1 mM EDTA buffer) were depicted in Fig. 2a. The dye showed characteristic absorption peaks at 591 and 429 nm attributed to the absorption of perylene chromophore and also, a small shoulder peak at 342 nm denoted to absorption of pyrene group attached to the bay positions of the perylene ring. **PDI-Pyr** dye gave two emission signals at 620 and 723 nm when the perylene chromophore was excited at 515 nm. Structurelessness of the emission bands and the large shoulder observed in the absorption spectra at the visible region in phosphate buffer at pH 6 might be attributed to the aggregation of the dye. When **PDI-Pyr** dye was excited at 317 nm which wavelength of pyrene group absorbs strongly, strong emission signals were observed at 381 and 394 nm which belong to pyrene monomer emission. Also, new emission peaks around 752 and 791 nm appeared. These new minor peaks were attributed to the charge-separated states generating from the electron transfer from the donor pyrene to the acceptor perylene core. No perylene emission signal was observed in phosphate buffer at pH 6. Solvatochromism with increasing solvent polarities on **PDI-Pyr** dye had been investigated in detail in our previous study [32].

Evaluation of Binding of the Ligands to G-quadruplex DNA

PDIs carrying with different positively-charged side chains interact with G-quadruplex, depending on side chain basicity [37–39]. The first dissociation constant related to indole ring

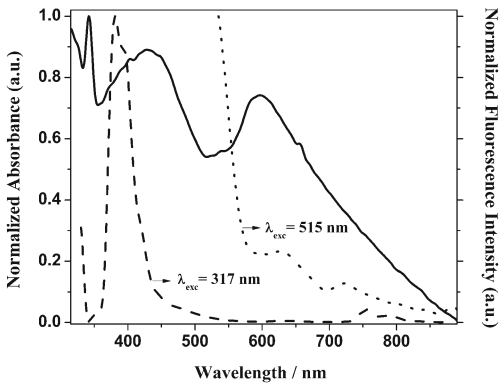

Fig. 2 Normalized visible absorption (*black line*), short-wavelength excited (λ_{exc}=317 nm) emission (*dashed line*) and long-wavelength excited (λ_{exc}=515 nm) emission spectra (*dotted line*) of **PDI-Pyr** in 170 mM phosphate buffer (70 mM potassium phosphate/100 mM KCl/1 mM EDTA) at pH 6

in **PDI-In** (pK_{a1}≈17.3) is doubled as compared to that of the value for phenol ring in **PDI-Ph** (pK_{a1}≈9.6, calculated with ACDLABS ChemSketch). Nitrogen and oxygen atoms in the rings are partially positively charged so that they show suitable feature to interact with G-quadruplex. Our studied PDIs contain nicotinic acid group which is partially positively charged at small fractions (pH 6) at one side of the molecule. Carboxylic acid group in the dyes loses a proton and changes into the carboxylate group with an acidity value of pK_{a2}≈2.6. Dissociation of the proton from the nitrogen atom in pyridine ring gives much lower acidity constant of pK_{a3}≈0.9, leading to unfavorable interaction side of the studied dyes for G-quadruplex sensitivity. However, carboxylic acid attached to pyridine ring enhances the solubility of the molecules in buffer solution. Isopropyl alkyl chains which are present on the other side of the molecule give rise to satisfactory solubility of the compounds.

Absorption spectra of **PDI-Ph**, **PDI-Pyr**, and **PDI-In** alone and interaction of various DNA structures in 170 mM phosphate buffer solution at pH 6 were given in Fig. 3a–c. No obvious spectral changes were observed from the absorption spectra of **PDI-Ph** between in the presence and absence of the nucleotides. Interaction of **PDI-In** with nucleotides causes absorbance decrease without any important wavelength shift, leading to an affinity for the studied ligands under experimental conditions. The most intrinsic absorbance decrease (≈14 %) was observed in the presence of ds-DNA at the wavelength of 602 nm. Remarkable enhancements in peak-to-valley ratio at maximum absorption band were observed from 6.54 in the absence of nucleotides to 21.5 and 17.3 in the presence of G4-DNA and G4′-DNA, respectively. Absorbance decrease seen below 400 nm in the presence of ss-DNA indicates the electrostatic interaction between the indole side of the dye and the polymeric backbone of thymine group.

In the presence of the nucleotides, the absorption spectrum of **PDI-Pyr** gave a marked red shift of 20 nm at 0–1 transition of perylene compared to the spectrum of nucleotide-free solution in phosphate buffer at pH 6. In pyrene absorption region, absorbance value of **PDI-Pyr** around 342 nm reduces by the addition of the nucleotides. Also, more gradual bathochromic shift from 591 nm to 604 nm were observed for **PDI-Pyr** in the presence of nucleotides. The peak-to-valley ratio at maximum absorption band enhanced from 1.35 in the absence of nucleotides to 1.51 and 1.40 in the presence of G4-DNA and G4′-DNA, respectively. These shifts could be explained by different interactions of PDI chromophores with nucleotides. Partially positive charged sites of PDIs cause electrostatic interactions with negatively charged phosphate groups. Also, this kind of binding may be explained by the π-π interaction between the aromatic rings and the π electron systems of guanines. Wengel and co-workers studied pyrene and perylene as fluorescence resonance energy transfer (FRET) pair when coupled to DNA and reported in 90 % FRET efficiency when the two chromophores were in close contact [40]. Also, pyrene-modified guanosine was used as a duplex-sensitive probe and

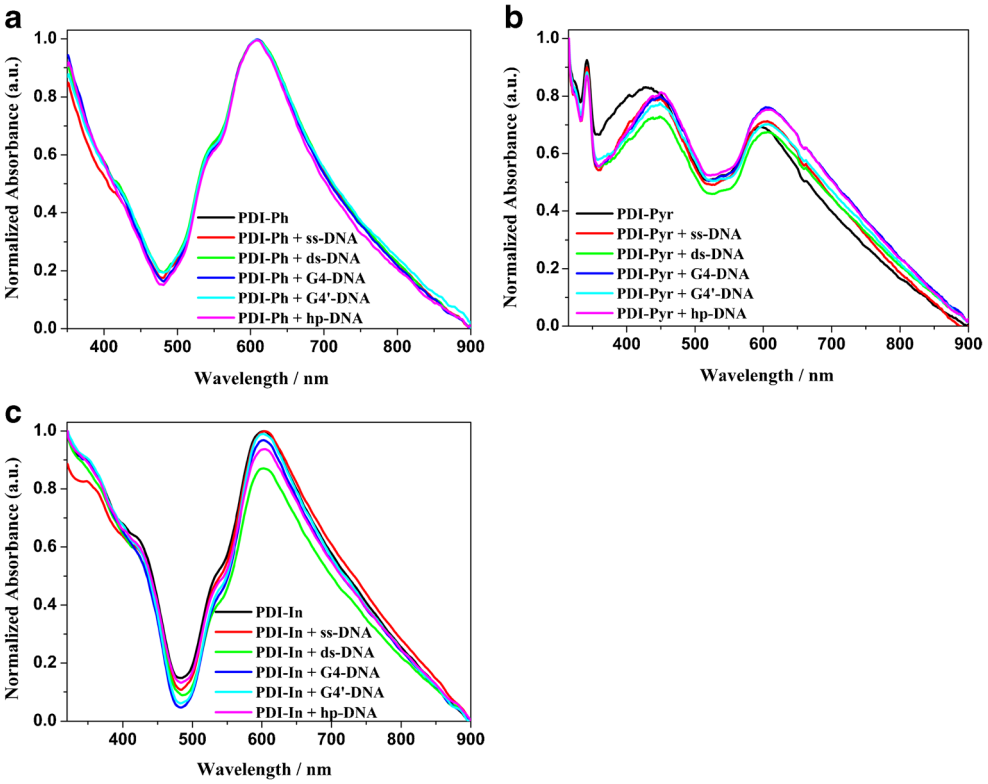

Fig. 3 Normalized UV–vis absorption spectra of 2 μM solutions of three PDI derivatives, **a PDI-Ph**, **b PDI-Pyr**, and **c PDI-In** in 170 mM phosphate buffer (70 mM potassium phosphate/100 mM KCl/1 mM EDTA) at pH 6 alone or in the presence of 2 μM solutions single-stranded DNA (ss-DNA), double-stranded-DNA (ds-DNA), intermolecular G-quadruplex DNA (G4-DNA), intramolecular G-quadruplex DNA (G4′-DNA) or dimeric hairpin quadruplex DNA (hp-DNA) structure

investigated in the DNA-mediated electron transfer processes in the literature [41]. Similar studies with perylenes revealed that these kind of ligands showed good binding selectivity to G-quadruplex by aggregating on the polymeric backbone of the DNAs [42]. Photoinduced energy or electron transfer process between the pyrene and perylene chromophores in **PDI-Pyr** molecule caused the rapid binding to the nucleotides. Also, ligand aggregation on DNA backbone might facilitate the binding selectivity to the nucleotides.

Singlet Oxygen Quantum Yields

Singlet oxygen quantum yields of the dyes were determined by the decay of the intensity of the *0–0* transition of DPBF. The solutions of 5 μM dyes in toluene/methanol (V/V = 99:1) containing 50 μM DPBF were aerated with a small aquarium pump for 5 min before irradiation. The decrease in the absorption of DPBF at 418 nm was monitored with a UV–visible spectrophotometer. Figure 4a displays the decrease in the absorbance of DPBF used as singlet oxygen scavenger. Also, Fig. 4b shows semi-logarithmic plots for the absorptions of DPBF versus time. The observed rate constants (k_{obs}) were calculated from $\ln(A_0/A)=k_{obs}\times t$ formula. Comparison of the slopes for the samples with the reference yielded the singlet oxygen quantum yield in a straightforward manner [43, 44] as given in Eq. 6.

$$\frac{\text{kobs(dye)}}{\text{kobs(ref)}} = \frac{\Phi\Delta(\text{dye})}{\Phi\Delta(\text{ref})} \tag{6}$$

With our photolysis system, Φ_Δ values of **PDI-Ph**, **PDI-Pyr**, and **PDI-In** were found to be about 0.52, 0.93 and 0.33, respectively. PDT effect of perylene and perylenequinonoid pigments have long been known in the literature, because they show high capacity of singlet O_2 production and also generate other reactive oxygen species which are important in PDT process [45–47]. Also, pyrene [48] and indole [49] structures are efficient photosensitizers generating singlet oxygen under irradiation. Activated indole-3-acetic acid under illuminating with red light in the presence of dyes enhanced the efficacy of photodynamic cancer therapy for hypoxic tumors by forming reactive cytotoxins rather than oxygen [50]. We could combine pyrene or indole group with PDI into a molecule with new functions. These new materials with higher capacity of singlet oxygen formation might be good candidates for PDT applications.

The energy of singlet state of oxygen lies 0.98 eV above the ground state [51]. The energy difference between the excited and ground state of **PDI-Pyr** dye (1.29 eV) [32] is much higher than that of singlet energy level of molecular oxygen so that singlet oxygen might be generated from energy transfer process. This energy transfer requires the spatial overlap of the orbital so that the excited state of the dye and the molecular oxygen are in close contact.

DNA Binding Experiments

Figure 5a shows the decrease in absorbance value of **PDI-Pyr** dye at 351 nm in titration experiment with the addition of G4-DNA or G4′-DNA to the phosphate buffer solution at pH 6. Figure 5b gives the static quenching data **PDI-Pyr** dye with G4-DNA or G4′-DNA structures at the pyrene excitation of 317 nm. At this wavelength, intramolecular energy or electron transfers occur in **PDI-Pyr** structure from pyrene donor to PDI acceptor. Marked enhancements of the dye emission with the addition of nucleotides were observed at the emission wavelength of pyrene monomer around 380–395 nm. When the dyes were titrated with nucleotides in the solution, excited states of pyrene (mostly pyrene cation) began to interact with the DNA strands and relaxed to its steady-state emission.

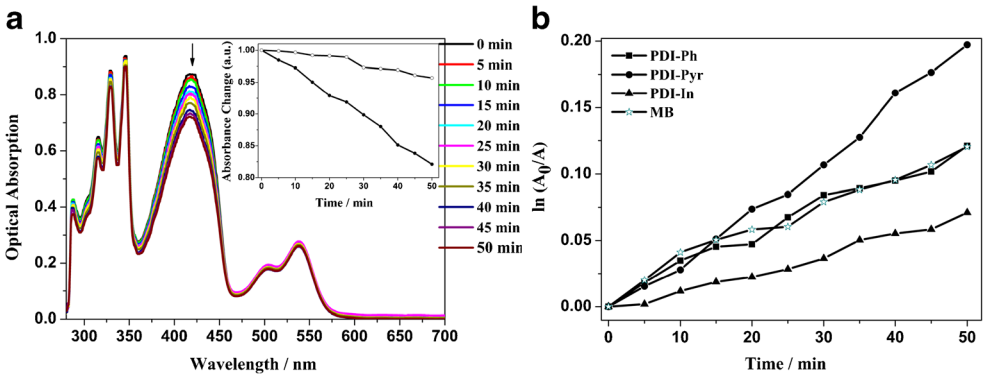

Fig. 4 **a** Decrease in absorption maxima of DPBF (50 μM) at 418 nm in toluene/methanol (V/V = 99:1) under illumination in the presence of 5 μM **PDI-Pyr** for 50 min after the solution was saturated with an air oxygen. Inset shows the **c**omparison of the absorption change of DPBF in dye-free solution (*light circle*) with in **PDI-Pyr** solution (*dark circle*) at the same conditions. **b** Semilogarithmic plots for the absorption decays of DPBF (50 μM) ($\ln A_0/A$) versus time at the same experimental conditions (**PDI-Ph**: 0.00226 X+0.00741 R^2: 0.98; **PDI-Pyr**: 0.00403 X − 0.00786 R^2: 0.99; **PDI-In**: 0.00144 X − 0.00362 R^2: 0.98; **MB**: 0.00220 X+ 0.01053 R^2: 0.98)

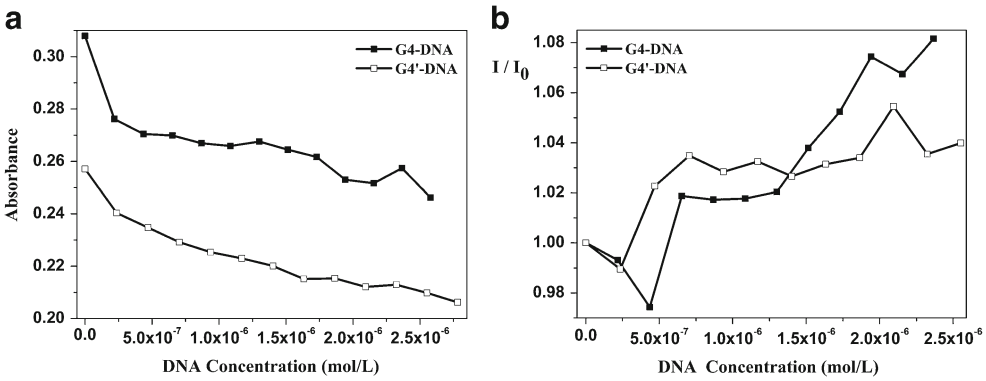

Fig. 5 **a** UV–vis absorption titration (λ=351 nm) and **b** fluorescence quenching spectra of 5 μM **PDI-Pyr** with addition of intermolecular G-quadruplex DNA (G4-DNA) or intramolecular G-quadruplex DNA (G4′-DNA) in 170 mM phosphate buffer (70 mM potassium phosphate/100 mM KCl/1 mM EDTA) at pH 6 (λ_{exc}= 317 nm)

Equation 7 was used to analyze the fluorescence quenching experiments using Stern–Volmer equation given below [52–55]:

$$\frac{I_0}{I} = 1 + k_q \times \tau_0 \times [Q] \tag{7}$$

where I_0 and I are the fluorescence intensities in the absence and presence of quenchers, respectively, and k_q is the quenching constant and τ_0 (6.4 ns) [32] is the radiative lifetime in the absence of the quencher. Quenching rate constants for titration experiments with G4-DNA and G4′-DNA structures were calculated to be about 5.16×10^5 and 5.92×10^5 $M^{-1}.s^{-1}$, respectively. These values were below the diffusion controlled quenching rates and indicated the energy transfer process from pyrene group to the DNA strands. Similar values were reported in the literature. Oligodeoxynucleoside fluorophores containing varied combinations of perylene and pyrene were prepared and the high efficiency of quenching was established by their large Stern–Volmer constants around 10^4–10^5 $M^{-1}.s^{-1}$ [56].

Also, we focused on the binding of **PDI-Pyr** dye to two different quadruplex sequences such as G4-DNA and G4′-DNA structures. Scatchard plots (Fig. 6) of the quenching data give the typical binding constants between the PDI dye and G4-DNA or G4′-DNA bases about 1.41×10^6 and 0.27×10^6 M^{-1}, respectively. Also, maximum number of **PDI-Pyr** molecules bound into G4-DNA and G4′-DNA were found to be 2 and 8, respectively. Similar binding constant values for PDI and pyrene derivatives interacting with oligonucleotides were obtained in literature survey. PDI derivatives as the complexes with $(TG_4T)_4$ gave the order of binding constant K_1 ranges between 10^5 and 10^7 M^{-1} [57]. Also, some pyrene derivatives showing binding activity to the targeted DNA structure gave the binding constants between 10^5 and 10^6 M^{-1} in the literature [58].

Figure 7 figures out the schematic illustration of possible singlet oxygen formation from the excited state of **PDI-Pyr** dye at the excitation wavelength of PDI. Energy transfer from the perylene core to the pyrene moieties was unlikely at the excitation wavelength of 510 nm, because S1 state of PDI chromophore was lower than S1 state of pyrene [32]. However, close contact between the spatial pyrene rings and the molecular oxygen in **PDI-Pyr** facilitates molecular oxygen localization [59]. Then, the most probable intermolecular energy transfer from PDI dye to the molecular oxygen produces the singlet oxygen. Also, pyrene is known as a good candidate as a fluorescence probe because of its complex forming ability with anionic ss-DNA or intercalation mode into the ds-DNA by change in its monomer or excimer emission [60–62]. Pyrene interacts with DNA mainly via the groove binding mode supported by the intercalation into the base pairs of DNA [58]. In **PDI-Pyr** structure, binding

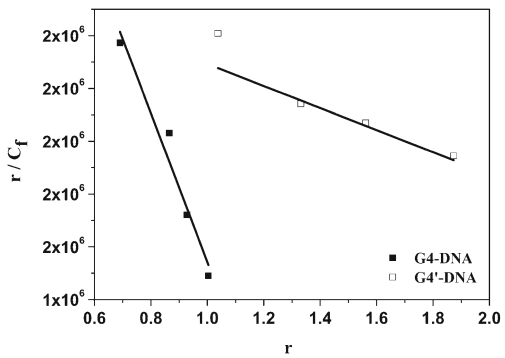

Fig. 6 Scatchard plots of r/C_f versus r for the absorption titrations of **PDI-Pyr** with G-quadruplex DNA (G4-DNA) (R^2: 0.95) or intramolecular G-quadruplex DNA (G4′-DNA) (R^2: 0.91)

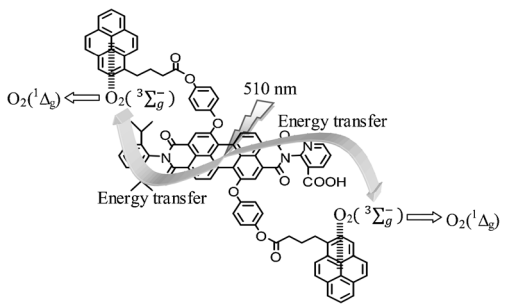

Fig. 7 Possible mechanism for explaining the singlet oxygen generation by **PDI-Pyr** sensitization

performance of pyrene group to DNA strands is an emerging approach of improving the PDI transfer to the targeted cancer tissue, then starting the PDT process with singlet oxygen.

Conclusion

The results of present study have demonstrated that phenyl-, pyrene-, or indol-modified PDIs could produce singlet oxygen with high quantum yields. **PDI-Pyr** and **PDI-In** dyes could bind to DNA from their side chains with substituted nitrogen or oxygen groups, presented in their cationic forms. Among the studied dyes, **PDI-Pyr** has shown good binding affinity to G-quadruplex structure with its excited state form of cationic pyrene. Fluorescence enhancements of **PDI-Pyr** emission observed in titration experiments are responsible for rapid binding of pyrene group to DNA, supporting the possibility of tumor-localizing property of PDI chromophore. This preliminary study has also indicated the delivery of the synthesized dyes into cancer cells via G-quadruplex binding, then the singlet oxygen could be produced with enhancing the specificity of PDT.

Acknowledgments Financial support from the Research Council of Celal Bayar University (BAP/2007-006 and 2010–050) was gratefully acknowledged.

References

1. Korbelik M, Naraparaju VR, Yamamato N (1997) Macrophage-directed immunotherapy as adjuvant to photodynamic therapy of cancer. Br J Cancer 75:202–207
2. Copper MP, Triesscheijn M, Tan IB, Ruevekamp MC, Stewart FA (2007) Photodynamic therapy in the treatment of multiple primary tumours in the head and neck, located to the oral cavity and oropharynx. Clin Otolaryngol 32:185–189
3. Phillips D (2010) Light relief: photochemistry and medicine. Photochem Photobiol Sci 9:1589–1596
4. Ikeda N, Usuda J, Kato H, Ishizumi T, Ichinose S, Otani K, Honda H, Furukawa K, Okunaka T, Tsutsui H (2011) New aspects of photodynamic therapy for central type early stage lung cancer. Laser Surg Med 43:749–754
5. Niemz MH (2007) Laser-tissue interactions fundamentals and applications. Springer, New York, pp 49–56
6. La Penna M, Alvarez MG, Yslas EI, Rivarola V, Durantini EN (2001) Photodynamic activity of 5,10,15,20-tetrakis (4-methoxyphenyl) porphyrin on the Hep-2 human carcinoma cell line: effect of light dose and wavelength range. Bioorg Chem 29:130–139
7. Milanesio ME, Alvarez MG, Silber JJ, Rivarola V, Durantini EN (2003) Photodynamic activity of monocationic and non-charged methoxyphenylporphyrin derivatives in homogeneous and biological media. Photochem Photobiol Sci 2:926–933
8. Schmidt R, Tanielian C (2000) Time-resolved determination of the quantum yield of singlet oxygen formation by tetraphenylporphine under conditions of very strong quenching. J Phys Chem A 104: 3177–3180
9. Yukruk F, Dogan AL, Canpinar H, Guc D, Akkaya EU (2005) Water-soluble green perylenediimide (PDI) dyes as potential sensitizers for photodynamic therapy. Org Lett 7:2885–2887
10. Jin YH, Hua JL, Wu WJ, Ma XM, Meng FS (2008) Synthesis, characterization and photovoltaic properties of two novel near-infrared absorbing perylene dyes containing benzo[e]indole for dye-sensitized solar cells. Synth Met 158:64–71
11. Zafer C, Kus M, Turkmen G, Dincalp H, Demic S, Kuban B, Teoman Y, Icli S (2007) New perylene derivative dyes for dye-sensitized solar cells. Sol Energy Mater Sol Cells 91:427–431
12. Chiu TL, Chuang KH, Lin CF, Ho YH, Lee JH, Chao CC, Leung MK, Wan DH, Li CY, Chen HL (2009) Low reflection and photosensitive organic light-emitting device with perylene diimide and double-metal structure. Thin Solid Films 517:3712–3716
13. Kim SH, Yang YS, Lee JH, Lee JI, Chu HY, Lee H, Oh J, Do LM, Zyung T (2003) Organic field-effect transistors using perylene. Opt Mater 21:439–443
14. Hayes RT, Wasielewski MR, Gosztola D (2000) Ultrafast photoswitched charge transmission through the bridge molecule in a donor-bridge-acceptor system. J Am Chem Soc 122:5563–5567
15. Langhals H, Karolin J, Johansson LBA (1998) Spectroscopic properties of new and convenient standards for measuring fluorescence quantum yields. J Chem Soc Faraday Trans 94:2919–2922
16. Chao CC, Leung MK, Su YO, Chiu KY, Lin TH, Shieh SJ, Lin SC (2005) Photophysical and electrochemical properties of 1,7-diaryl-substituted perylene diimides. J Org Chem 70:4323–4331
17. Zhao Q, Zhang HY (2005) Singlet-oxygen-generating activity of deuterated perylenequinonoid pigments. Dyes Pigments 66:15–17
18. Icli S, Demic S, Dindar B, Doroshenko AO, Timur C (2000) Photophysical and photochemical properties of a water-soluble perylene diimide derivative. J Photochem Photobiol A Chem 136: 15–24
19. Dincalp H, Icli S (2006) Photoinduced electron transfer-catalyzed processes of sulfoamino perylene diimide under concentrated sun light. Sol Energy 80:332–346
20. Karapire C, Zafer C, Icli S (2004) Studies on photophysical and electrochemical properties of synthesized hydroxy perylenediimides in nanostructured titania thin films. Synth Met 145:51–60
21. Kerwin SM, Chen G, Kern JT, Thomas PW (2002) Perylene diimide G-quadruplex DNA binding selectivity is mediated by ligand aggregation. Bioorg Med Chem Lett 12:447–450
22. Kern JT, Thomas PW, Kerwin SM (2002) The relationship between ligand aggregation and G-quadruplex DNA selectivity in a series of 3,4,9,10-perylenetetracarboxylic acid diimides. Biochemistry 41: 11379–11389
23. Fedoroff OY, Salazar M, Han HY, Chemeris VV, Kerwin SM, Hurley LH (1998) NMR-based model of a telomerase-inhibiting compound bound to G-quadruplex DNA. Biochemistry 37:12367–12374
24. Dai JX, Carver M, Yang DZ (2008) Polymorphism of human telomeric quadruplex structures. Biochimie 90:1172–1183
25. Nakamura TM, Morin GB, Chapman KB, Weinrich SL, Andrews WH, Lingner J, Harley CB, Cech TR (1997) Telomerase catalytic subunit homologs from fission yeast and human. Science 277:955–959
26. Haider SM, Neidle S, Parkinson GN (2011) A structural analysis of G-quadruplex/ligand interactions. Biochimie 93:1239–1251
27. Neidle S (2010) Human telomeric G-quadruplex: the current status of telomeric G-quadruplexes as therapeutic targets in human cancer. FEBS J 277:1118–1125
28. Bugaj AM (2011) Targeted photodynamic therapy - a promising strategy of tumor treatment. Photochem Photobiol Sci 10:1097–1109
29. Shieh YA, Yang SJ, Wei MF, Shieh MJ (2010) Aptamer-based tumor-targeted drug delivery for photodynamic therapy. ACS Nano 4:1433–1442
30. Abdel-Shafi AA, Worrall DR, Wilkinson F (2001) Singlet oxygen formation efficiencies following quenching of excited singlet and

triplet states of aromatic hydrocarbons by molecular oxygen. J Photochem Photobiol A Chem 142:133–143
31. Criado S, Martire D, Allegretti P, Furlong J, Bertolotti SG, La Falce E, Garcia N (2002) Singlet molecular oxygen generation and quenching by the antiglaucoma ophthalmic drugs, Timolol and Pindolol. Photochem Photobiol Sci 1:788–792
32. Dincalp H, Kizilok S, Icli S (2010) Fluorescent macromolecular perylene diimides containing pyrene or indole units in bay positions. Dyes Pigments 86:32–41
33. Wetzler DE, Garcia-Fresnadillo D, Orellana G (2006) A clean, well-defined solid system for photosensitized O-1(2) production measurements. Phys Chem Chem Phys 8:2249–2256
34. Han HY, Cliff CL, Hurley LH (1999) Accelerated assembly of G-quadruplex structures by a small molecule. Biochemistry 38:6981–6986
35. Anantha NV, Azam M, Sheardy RD (1998) Porphyrin binding to quadruplexed T(4)G(4). Biochemistry 37:2709–2714
36. Wei CY, Jia GQ, Zhou J, Han GY, Li C (2009) Evidence for the binding mode of porphyrins to G-quadruplex DNA. Phys Chem Chem Phys 11:4025–4032
37. Kern JT, Kerwin SM (2002) The aggregation and G-quadruplex DNA selectivity of charged 3,4,9,10-perylenetetracarboxylic acid diimides. Bioorg Med Chem Lett 12:3395–3398
38. Rossetti L, Franceschin M, Schirripa S, Bianco A, Ortaggi G, Savino M (2005) Selective interactions of perylene derivatives having different side chains with inter- and intramolecular G-quadruplex DNA structures. A correlation with telomerase inhibition. Bioorg Med Chem Lett 15:413–420
39. Samudrala R, Zhang X, Wadkins RM, Mattern DL (2007) Synthesis of a non-cationic, water-soluble perylenetetracarboxylic diimide and its interactions with G-quadruplex-forming DNA. Bioorg Med Chem 15:186–193
40. Lindegaard D, Madsen AS, Astakhova IV, Malakhov AD, Babu BR, Korshun VA, Wengel J (2008) Pyrene-perylene as a FRET pair coupled to the N2′-functionality of 2′-amino-LNA. Bioorg Med Chem 16:94–99
41. Wanninger-Weiss C, Valis L, Wagenknecht HA (2008) Pyrene-modified guanosine as fluorescent probe for DNA modulated by charge transfer. Bioorg Med Chem 16:100–106
42. Dincalp H, Avcibasi N, Icli S (2007) Spectral properties and G-quadruplex DNA binding selectivities of a series of unsymmetrical perylene diimides. J Photochem Photobiol A Chem 185:1–12
43. Serra AC, Pineiro M, Gonsalves A, Abrantes M, Laranjo M, Santos AC, Botelho MF (2008) Halogen atom effect on photophysical and photodynamic characteristics of derivatives of 5,10,15,20-tetrakis(3-hydroxyphenyl)porphyrin. J Photochem Photobiol B Biol 92:59–65
44. Scalise I, Durantini EN (2004) Photodynamic effect of metallo 5-(4-carboxyphenyl)-10,15,20-tris(4-methylphenyl) porphyrins in biomimetic AOT reverse micelles containing urease. J Photochem Photobiol A Chem 162:105–113
45. Zhang HY, Liu W, Liu WZ, Xie JL (2001) Photosensitization of hypomycin B−A novel perylenequinonoid pigment with only one intramolecular hydrogen bond. Photochem Photobiol 74:191–195
46. Waser M, Falk H (2007) Towards second generation hypericin based photosensitizers for photodynamic therapy. Curr Org Chem 11:547–558
47. Liu X, Xie J, Zhang LY, Chen HX, Gu Y, Zhao JQ (2009) A novel hypocrellin B derivative designed and synthesized by taking consideration to both drug delivery and biological photodynamic activity. J Photochem Photobiol B 94:171–178
48. Schweitzer C, Schmidt R (2003) Physical mechanisms of generation and deactivation of singlet oxygen. Chem Rev 103:1685–1757
49. Ranby B, Rabek JF (1978) Singlet oxygen: reactions with organic compounds and polymers. Wiley, New York, pp 48–53
50. Folkes LK, Wardman P (2003) Enhancing the efficacy of photodynamic cancer therapy by radicals from plant auxin (indole-3-acetic acid). Cancer Res 63:776–779
51. Sato C, Kikuchi K, Okamura K, Takahashi Y, Miyashi T (1995) New aspects on fluorescence quenching by molecular-oxygen. 2. inhibition of long-distance electron-transfer in acetonitrile. J Phys Chem 99:16925–16931
52. Lakowicz JR (1999) Principles of fluorescence spectroscopy. Kluwer Academic Pub, New York, pp 239–242
53. Gok E, Ates S (2003) Fluorimetric determination of thyroxine hormone with Eu(III)-(pyridine-2,6-dicarboxylate) tris complex. J Fluoresc 13:221–225
54. Gok E (2013) Investigation of binding properties of umbelliferone (7Hydroxycoumarin) to lysozyme. J Fluoresc 23:333–338
55. Yargi O, Ugur S, Pekcan O (2013) Oxygen diffusion into multiwalled carbon nanotube doped polystrene latex films using fluorescence technique. J Fluoresc 23:357–366
56. Teo YN, Wilson JN, Kool ET (2009) Polyfluorophore labels on DNA: dramatic sequence dependence of quenching. Chem Eur J 15:11551–11558
57. Casagrande V, Alvino A, Bianco A, Ortaggi G, Franceschin M (2009) Study of binding affinity and selectivity of perylene and coronene derivatives towards duplex and quadruplex DNA by ESI-MS. J Mass Spectrom 44:530–540
58. Li L, Lu J, Xu CZ, Li HH, Yang XD (2012) Studies on the interaction mechanism of pyrene derivatives with human tumor-related DNA. Molecules 17:14159–14173
59. Abdel-Shafi AA, Worrall DR (2005) Mechanism of the excited singlet and triplet states quenching by molecular oxygen in acetonitrile. J Photochem Photobiol A Chem 172:170–179
60. Yang LY, Zhao M, Zhang RC, Dong J, Zhang T, Zhan XW, Wang GJ (2012) Synthesis and fluorescence study of a quaternized copolymer containing pyrene for DNA-hybridization detection. Chem Phys Chem 13:4099–4104
61. Chen CY, Ito Y, Chiu YC, Wu WC, Higashihara T, Ueda M, Chen WC (2012) Design and synthesis of new cationic water-soluble pyrene containing dendrons for DNA sensory applications. J Polym Sci A1(50):297–305
62. Wu CC, Wang CM, Yan L, Yang CJ (2009) Pyrene excimer nucleic acid probes for biomolecule signaling. J Biomed Nanotechnol 5:495–504